AD-A104 937 NAVAL RESEARCH LAB WASHINGTON DC F/G 20/9
THRESHOLD CRITERIA FOR A SPACE-SIMULATION BEAM-PLASMA-DISCHARGE--ETC(U)
SEP 81 E P SZUSZCZEWICZ, K PAPADOPOULOS
UNCLASSIFIED NRL-MR-4608 NL

END
DATE FILMED
10-81
DTIC

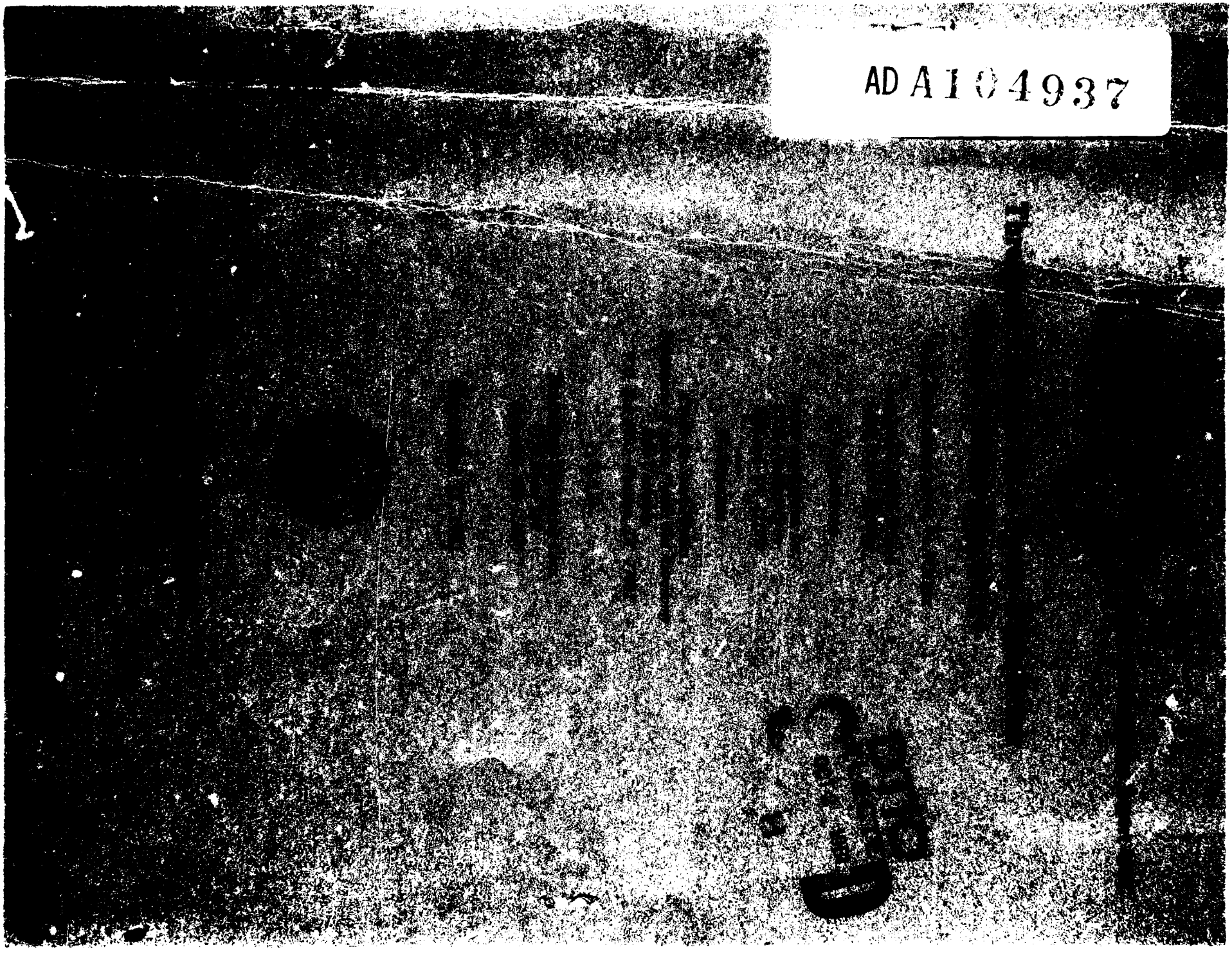

SECURITY CLASSIFICATION OF THIS PAGE (When Data Entered)

REPORT DOCUMENTATION PAGE

READ INSTRUCTIONS BEFORE COMPLETING FORM

1. REPORT NUMBER: NRL Memorandum Report 4608	2. GOVT ACCESSION NO.: AD-A104937
3. RECIPIENT'S CATALOG NUMBER:	
4. TITLE (and Subtitle): THRESHOLD CRITERIA FOR A SPACE-SIMULATION BEAM-PLASMA-DISCHARGE	5. TYPE OF REPORT & PERIOD COVERED: Interim report on a continuing NRL problem.
	6. PERFORMING ORG. REPORT NUMBER:
7. AUTHOR(s): E. P. Szuszczewicz, K. Papadopoulos, W. Bernstein*, C. S. Lin, and D. N. Walker	8. CONTRACT OR GRANT NUMBER(s): NASA/NOAA Cont. NA79RAE00039; NASA Grant NAGW-69; Rice Univ. sub-cont. NAS 8-33777-1
9. PERFORMING ORGANIZATION NAME AND ADDRESS: Naval Research Laboratory, Washington, DC 20375	10. PROGRAM ELEMENT, PROJECT, TASK AREA & WORK UNIT NUMBERS: 61153N; RR033-02-44; 41-0949-0-1; 41-0951-0-0
11. CONTROLLING OFFICE NAME AND ADDRESS: Office of Naval Research, Arlington, VA 22217	12. REPORT DATE: September 30, 1981
	13. NUMBER OF PAGES: 27
14. MONITORING AGENCY NAME & ADDRESS (if different from Controlling Office): Department of Commerce/NOAA, Boulder, Colorado 80302	15. SECURITY CLASS. (of this report): UNCLASSIFIED
	15a. DECLASSIFICATION/DOWNGRADING SCHEDULE:

16. DISTRIBUTION STATEMENT (of this Report)

Approved for public release; distribution unlimited.

17. DISTRIBUTION STATEMENT (of the abstract entered in Block 20, if different from Report)

18. SUPPLEMENTARY NOTES

*Present address: Science Applications, Inc., 1710 Goodrich Drive, McLean, VA 22102

**Present address: Center for Space Physics, Dept. of Space Physics and Astronomy, Rice University, P. O. Box 1892, Houston, TX 77001

†Present address: Bendix Field Engineering Corp., 9250 Route 108, Columbia, MD 21045

19. KEY WORDS (Continue on reverse side if necessary and identify by block number)

Plasma Physics
Beam plasma discharge (BPD)
Beam plasma ignition
Pulsed probe (P^3)
Space-simulation vacuum chamber

20. ABSTRACT (Continue on reverse side if necessary and identify by block number)

We have conducted an experimental and theoretical study of the threshold characteristics of a space-simulation beam-plasma-discharge (BPD) with emphasis on density profiles and density-dependent ignition criteria. The study included various beam-plasma conditions covering beam currents from 8 to 85 ma, beam energies from 0.8 to 2.0 keV and magnetic fields at 0.9 and 1.5 gauss. The study included experimental determinations of radial profiles of electron density for each of the selected conditions extending from a low-density per-BPD state to a strong BPD condition. At BPD threshold it was

(Continues)

DD FORM 1 JAN 73 1473 EDITION OF 1 NOV 65 IS OBSOLETE
S/N 0102-014-6601

SECURITY CLASSIFICATION OF THIS PAGE (When Data Entered)

20. ABSTRACT (Continued)

determined that $3.9 \lesssim \omega_p/\omega_c \lesssim 5.8$ was the density-dependent ignition criterion. The experimental results are shown to agree with detailed model calculations which consider the BPD to be produced by large amplitude electron plasma waves resulting from the beam-plasma interaction.

CONTENTS

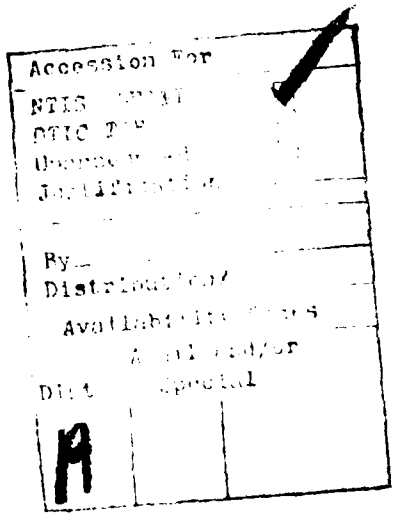

THRESHOLD CRITERIA FOR A SPACE-SIMULATION BEAM-PLASMA-DISCHARGE

I. INTRODUCTION

A cold electron beam, propagating through a weakly ionized plasma will, under proper conditions, produce a modified beam-plasma state known as the Beam-Plasma-Discharge (BPD). This discharge state has received considerable attention in recent years as a result of increased interest in mechanisms for vehicle neutralization during spaceborne accelerator experiments (Bernstein, et al., 1980; Cambou, et al., 1978), enhanced beam-plasma ionization processes (Bernstein, et al., 1978), and in general single-particle or collective phenomena initiated by beams injected into neutral gas and charged-particle environments (Hess et al., 1971; Winckler, et al., 1975; Hendrickson and Winckler 1976; Cambou, et al., 1975; Munson and Kellogg 1978a; Szuszczewicz, et al., 1979; Jost et al., 1980; Winckler 1980).

The BPD appears at a critical energetic-electron-beam current I_B^c, with the transition from single-particle behavior ($I_B < I_B^c$, pre-BPD) to collective processes ($I_B > I_B^c$, solid-BPD) described as follows for conditions in which the plasma is created by the beam itself:

(i) As an electron beam linearly interacts with a neutral gas, it collisionally produces a plasma with a density that varies directly with the magnitude of the beam current for a fixed beam energy.

(ii) As the beam current is increased to a critical value, I_B^c, a two-stream instability sets in and the electric fields of the excited waves heat the electrons to energies comparable to the ionization energy. The "heated" electrons create an enhanced ionization process which results in an avalanche breakdown, the BPD.

Manuscript submitted July 14, 1981.

Bernstein et al., (1979) have reported the dependence of this critical current, I_B^c, on various experimental parameters as

$$I_B^c \propto \frac{V_B^{3/2}}{B^{0.7} PL} \qquad (1)$$

where V_B, B, P and L are the beam energy (voltage), the superimposed magnetic field, the ambient neutral pressure, and the beam length (gun-to-collector distance), respectively. While the $I_B^c = I_B^c (V_B, B, P, L)$ relationship was established among the controlling system parameters, a clear dependence on plasma density was expected, with early thoughts suggesting that $\omega_p \gtrsim \omega_c$ satisfied ignition threshold criteria (Bernstein, et al., 1979; Getty and Smullin, 1963). We have since had the opportunity to test these ideas under various beam-plasma conditions. Our results include:

(i) Time-delay data and associated analyses indicating that BPD ignition does indeed occur at a critical density,

(ii) Direct measurements of plasma density near ignition threshold with determinations of ω_p/ω_c, and

(iii) A theoretical analysis which predicts the critical density criterion.

In subsequent sections, we present the experimental and theoretical details which establish the density-dependent threshold conditions for BPD at $3.9 \lesssim \omega_p/\omega_c \lesssim 5.8$.

II. EXPERIMENT CONFIGURATION AND RESULTS

The experiment was conducted in a large vacuum chamber facility at the NASA Johnson Space Flight Center with an experimental configuration similar to those employed in earlier investigations (Bernstein et al., 1979). The

configuration is illustrated in Figure 1 with specific emphasis on the pulsed plasma probe measurement and the associated procedure for ω_p/ω_c determinations. Not shown are the previously described diagnostics (Bernstein et al., 1979; Jost et al., 1980) including the 3914Å scanning photometer, the segmented current collector, the energetic electron electrostatic analyzer, and the remote wave detection antenna and spectrum analyzer system. The beam was generated by a tungsten-cathode Pierce-type diode gun, mounted on a position-controlled cart. In all cases the beam was injected parallel to the magnetic field $\bar{B}$ and terminated on a 3 x 3 m target suspended about 20 m above the gun aperture. A combination of coil current and the Earth's magnetic field established the B-field at selected levels up to 1.5 gauss.

In most cases the beam was injected into a neutral gas with no pre-beam plasma; however the experimental investigation included two cases in which the chamber was filled with a plasma created by a Kauffman-type argon ion thruster. In these cases the pre-beam plasma density was lower than the critical density at BPD ignition.

The investigation was conducted in two stages. First, pulsed-gun experiments were carried out to test the concept of a density-dependent threshold condition against the original ideas of Getty and Smullin (1963). After the concepts check, a series of direct density measurements were conducted to quantitatively establish the density criteria. We describe the results in the order in which the experiments were conducted.

Time-Delay Arguments for N_e^c

In pulsed-beam experiments with $I_B >> I_B^c$, Getty and Smullin (1963) identified three sequential phases in the temporal evolution into the BPD: 1) a quiescent stable

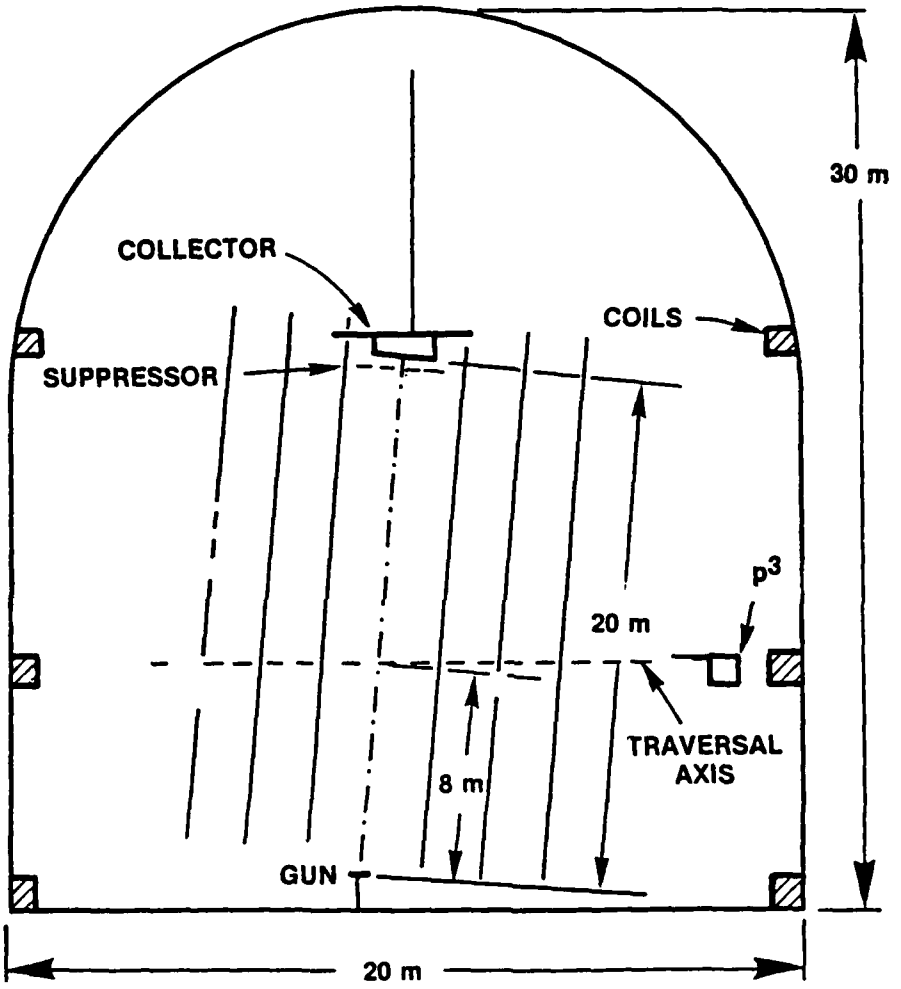

Fig. 1 — Experiment configuration

period, 2) an intermediate period during which the gross features of the beam remained unchanged but waves with $f \approx f_{ce}$ were present, and 3) BPD ignition. They suggested that phases 1 and 2 corresponded to the time required for buildup of the ambient density to a critical value...a value at which the BPD ignited. To test this concept in the space-simulation beam-plasma efforts at the JSC facility a series of pulsed beam measurements were performed to study the temporal evolution of the BPD in the configuration shown in Fig. 1. All diagnostics sensitive to the transition to BPD demonstrated identical time delays between beam current initiation and BPD ignition. At low pressure ($< 4(10^{-6})$ torr) the Getty and Smullin phase 2 (characterized by $f \approx f_{ce}$ waves) was clearly evident. Figure 2 shows the measured delay times as a function of beam current with values ranging from 0.1-20 msec. The results in Figure 2 can be understood in terms of a simple time-dependent model. If it is assumed that the plasma loss rate is proportional to its density, then the temporal buildup of plasma by electron-neutral collisions is given by

$$N_e = \frac{PL}{\lambda} \left(1 - \exp\left[- \frac{\lambda}{L} \, t \right]\right). \tag{2}$$

Equation (2) follows directly from Getty and Smullin (1963) as the solution to

$$\frac{dN_e}{dt} = P - \frac{\lambda}{L} \, N_e \tag{3}$$

where $P = I_B \, \sigma N_o / eA$ is the electron-ion pair production rate, λ/L is the loss rate, σ the electron impact ionization cross section, N_o the neutral density and A the beam cross section. At short times, the density will increase linearly

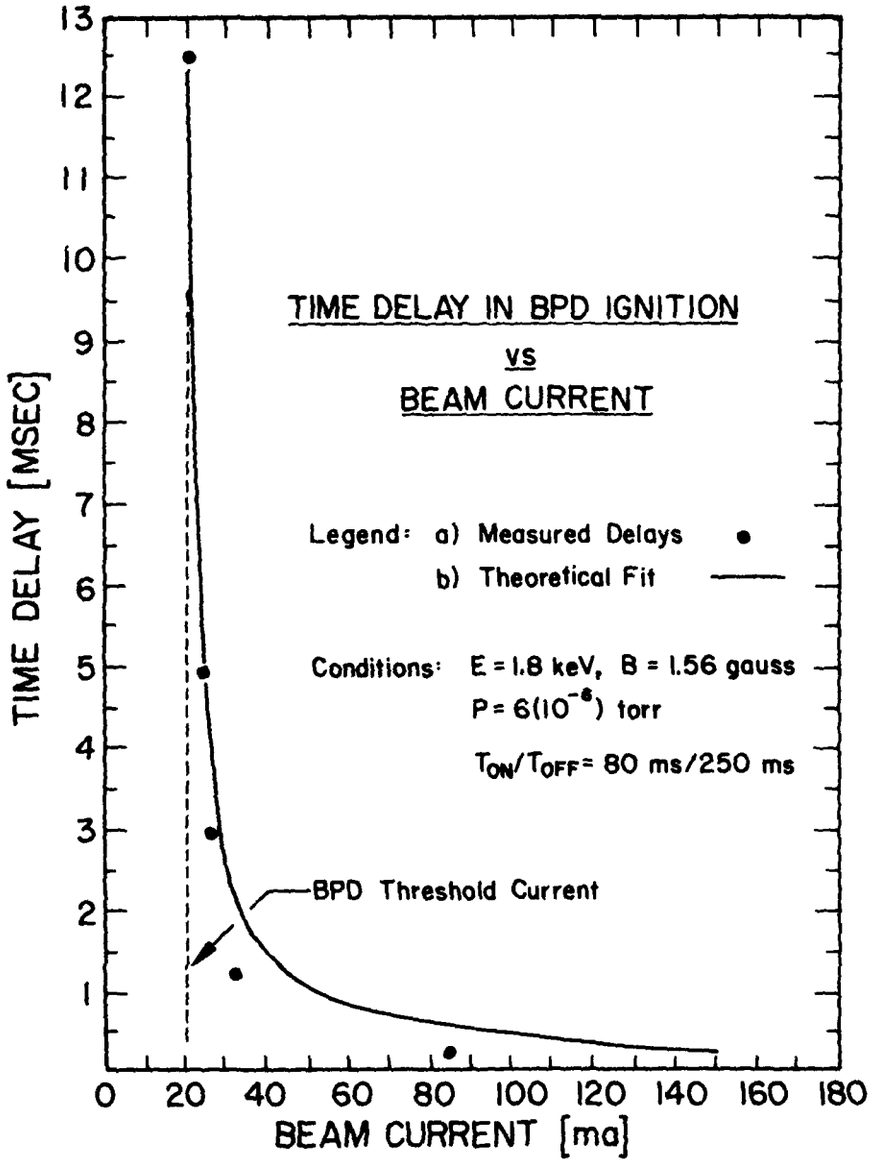

Fig. 2 — Time delay in the ignition of the beam-plasma-discharge with threshold current at 20 ma

with time (N_e = Pt) and at longer times the density will approach the time-independent value $N_e = PL/\lambda$. For $I_B \gtrsim I_B^c$ relatively long delay times should be observed with a rapid decrease in t_d as I_B is increased. This is exactly the behavior demonstrated in Figure 2, where Equation (2) has been normalized to the data. The good agreement between the simple model calculations and the experimental results supports the concept of a critical density threshold for BPD ignition, but the normalization procedure provides little measure for an absolute value of N_e^c. Specific determinations of the critical density threshold criteria are detailed in the next two sections.

Direct Measurements of Critical Density

To quantitatively establish the density-dependent threshold criterion for the ignition of a space-simulation BPD, emphasis was placed on the direct measurement of plasma density profiles over a range of beam-plasma conditions covering beam currents from 8 to 85 ma, beam energies from 0.8 to 2.0 keV and magnetic fields at 0.9 and 1.5 gauss. The procedure involved experimental determinations of radial profiles of electron density for each of the selected conditions extending from a low-pre-BPD state to a strong BPD condition. The experimental configuration, illustrated in Figure 1, involved a pair of pulsed-plasma-probes mounted on a radial traversal mechanism positioned at approximately 8 m above the injection point of the beam. Each of the probes provided simultaneous measurements of electron density N_e, temperature T_e, plasma potential V_ω, and density fluctuation power spectra δN_e ($\rightarrow P_n(k)$) with capabilities for the associated diagnostics in a dynamic plasma environment and under test conditions which could contaminate electrode surfaces (Holmes and Szuszczewicz, 1975, 1981; Szuszczewicz and Holmes 1975,1976).

The plasma density measurements were made for seven different conditions, each identified by pre-selected values for V_B, B, P and the existence or non-existence of a pre-beam plasma. For each condition a steady state value for I_B was set, the traversal mechanism exercised, and an electron density profile was recorded. A sample profile collected under pre-BPD conditions, is presented in Figure 3. The abscissa is time relative to the start of the radial traversal and the ordinate is relative electron density as determined by baseline electron-saturation currents collected by the E-probe. (The second in the two-probe configuration was defined as the I-probe because the associated baseline currents were collected in the ion-saturation portion of the probe's current-voltage characteristic (Holmes and Szuszczewicz, 1975, 1981).) At the start of each traversal the probe was at its outermost position relative to the center of the chamber. As time increased the probe was moved into and through the beam; at maximum penetration toward the chamber center, the traversal system was reversed, allowing a second measurement of the density profile as the probe moved back to its original outermost position. With this procedure the probe's maximum penetration toward the chamber center is identified by the symmetry point in the "double" profile. The symmetry in the "double" profile provided confidence that beam-plasma conditions were unchanged during the measurement.

Absolute electron densities were determined by standard P^3 analysis procedures summarized graphically in Figure 4. The technique provides a high-frequency (10^3 Hz in this experiment) determination of relative electron density through the direct measurement of baseline electron-saturation-currents. Simultaneously, the technique generates a "conventional"

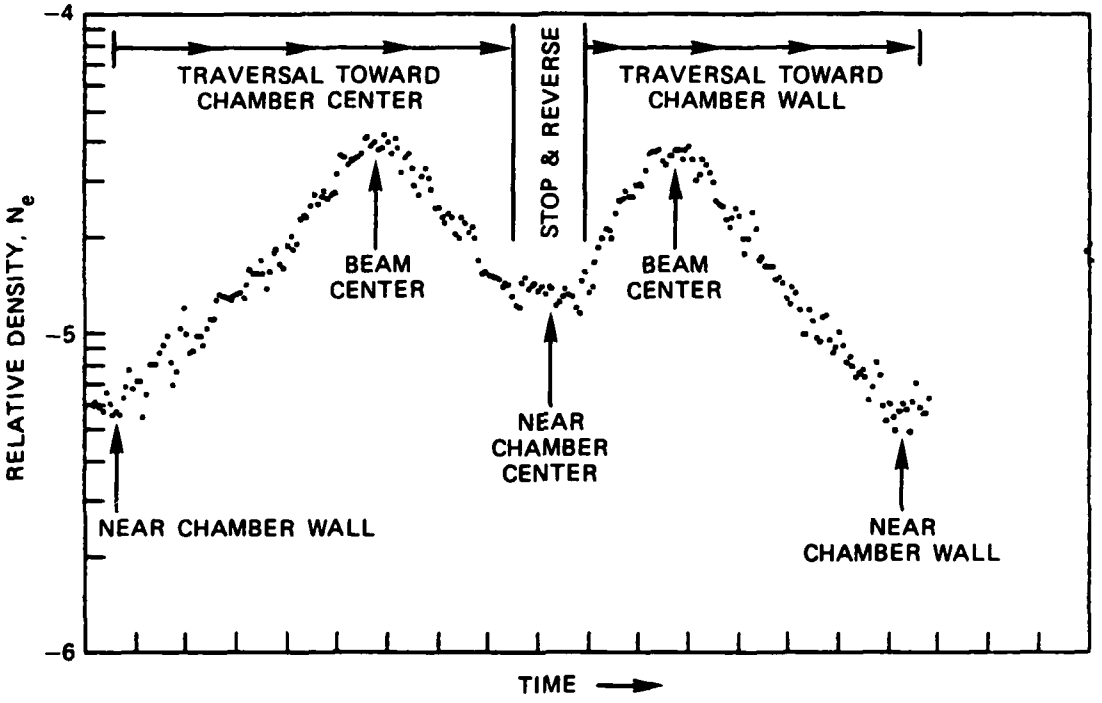

Fig. 3 — Radial profile of relative electron density under pre-BPD conditions. Run #57, (I_B, V_B, B) = (7 ma, 1.3 keV, 0.9g). The figure shows two cuts through the beam-plasma profile, as time increases from left-to-right the plasma density probe moves into and through the beam center, then reverses and passes through the beam a second time. The symmetry verifies that beam-plasma conditions were stable during the execution of the radial traversal.

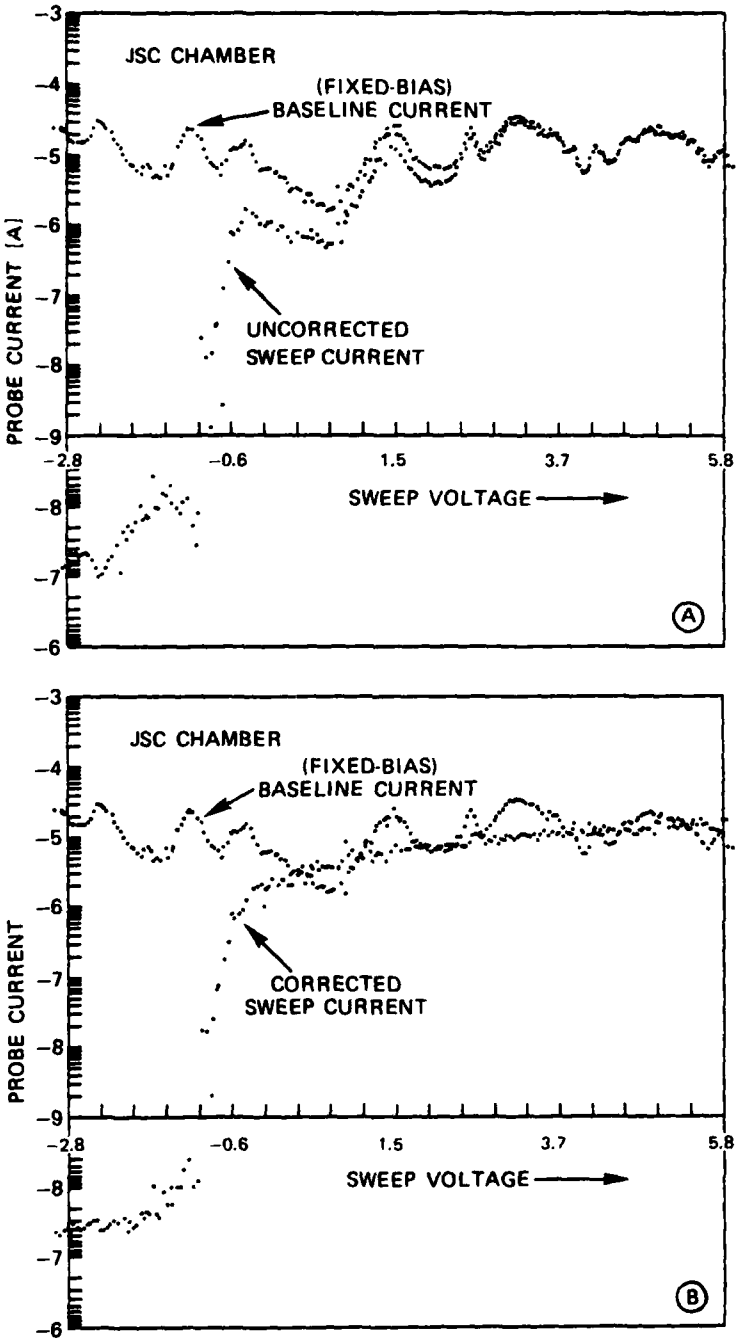

Fig. 4 — Sample of raw probe data (3A) showing the effects of density fluctuations (baseline electron-saturation-currents) on the probe's current-voltage characteristic (sweep currents). 3B shows the "corrected" characteristic that results when density fluctuations have been unfolded. The electron saturation portion of the characteristic is then amenable to conventional analyses for determination of N_e (see text).

Langmuir probe characteristic. The relative density fluctuations (as indicated by the variations in the baseline current) are then unfolded from the raw, uncorrected probe characteristic (Fig. 4A) yielding a smooth, corrected curve (Fig. 4B) to which conventional N_e-analysis procedures (Chen, 1965; Szuszczewicz and Holmes, 1977) are applied. This procedure was utilized for all beam-plasma conditions included in this investigation.

Complete profile information and associated plasma wave signatures are presented for two independent conditions in Figures 5 and 6. (Note: Because of changes in plasma potential, the relative density profiles do not maintain the same scaling to absolute values from run-to-run.) For values of (V_B,B) = (1.3 keV, 0.9G) and (2.0 keV, 1.5G) in Figures 5 and 6, respectively, the beam current I_B was stepped through a sequence allowing for complete coverage of conditions which encompassed pre-, threshold-, and solid-BPD. Because $I_B^c = I_B\ (V_B,B,P,L)$ is known to exhibit hysteresis as I_B is varied about the critical value I_B^c, the following procedure was utilized in the step-wise selection of beam current levels:

(i) With V_B fixed, I_B was steadily increased in a "search" mode to determine an approximate value for I_B^c.

(ii) I_B was reset to zero, then increased slowly to I_B^c with careful observation of the RF spectrum. Threshold was defined as that level at which the RF spectrum was in transition from its pre- BPD signature (flat spectrum at high frequencies, $f \gtrsim f_p$) to its solid-BPD characteristic (intense features at $f \gtrsim f_p$). At this transition level (defined here as threshold) the beam-plasma system oscillated between its two states at a repetition frequency generally observed to be no greater than several Hertz. If the RF spectrum "locked-up" in a characteristically stable RF BPD signature, step "(ii)" was restarted and the previous I_B^c level more carefully approached.

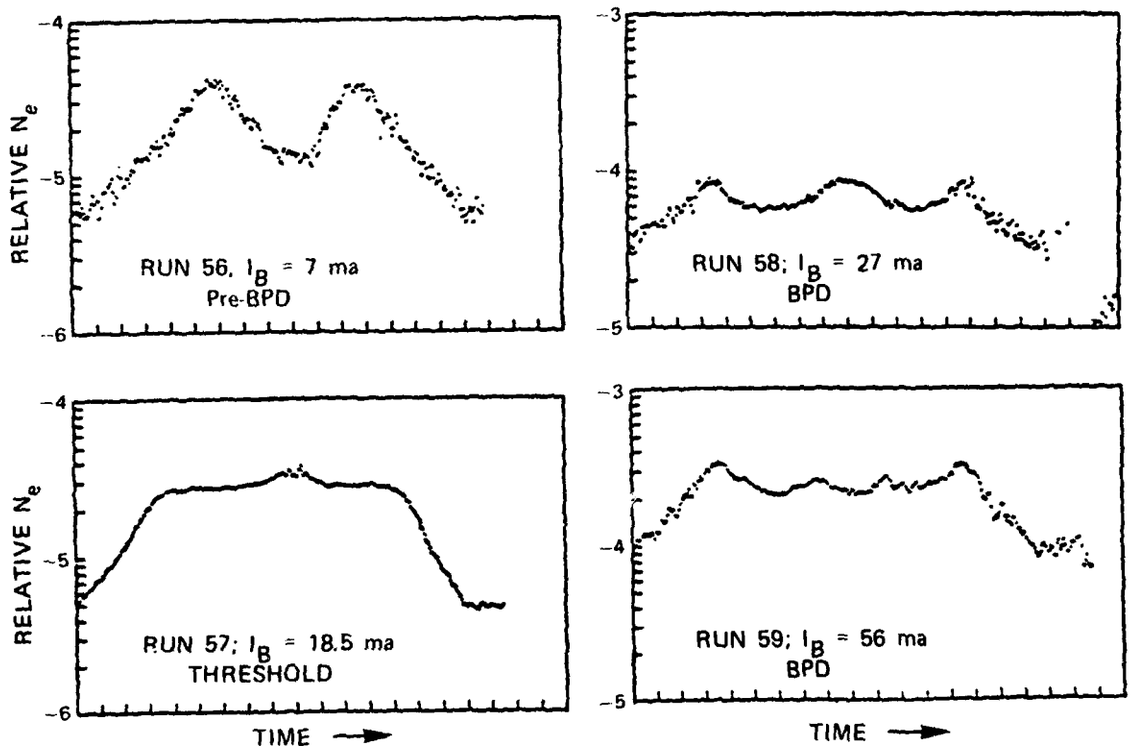
RELATIVE N_e
−4
−5
−6
RUN 56, I_B = 7 ma
Pre-BPD
−3
−4
−5
RUN 58; I_B = 27 ma
BPD
RELATIVE N_e
−4
−5
−6
RUN 57; I_B = 18.5 ma
THRESHOLD
−3
−4
−5
RUN 59; I_B = 56 ma
BPD
TIME
TIME

(a)

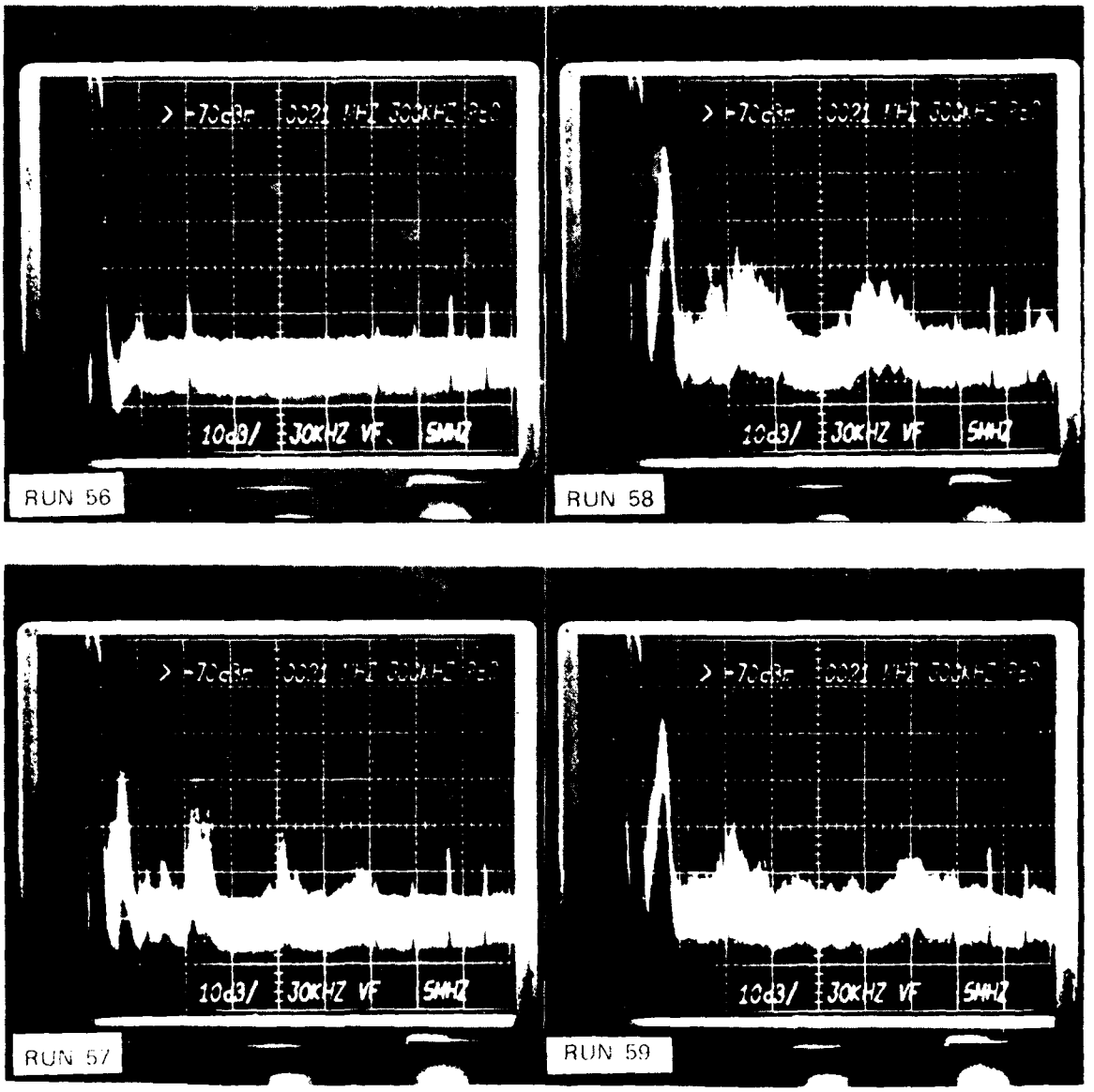

(b)

Fig. 5 – Sequence of relative plasma density profiles (Fig. 4A) and associated plasma wave signatures (Fig. 4B) for increasing values of beam current I_B at a fixed condition (V_B,B) = (1.3 keV, 0.9g) encompassing runs 56 through 83 (pre-BPD through solid-BPD).

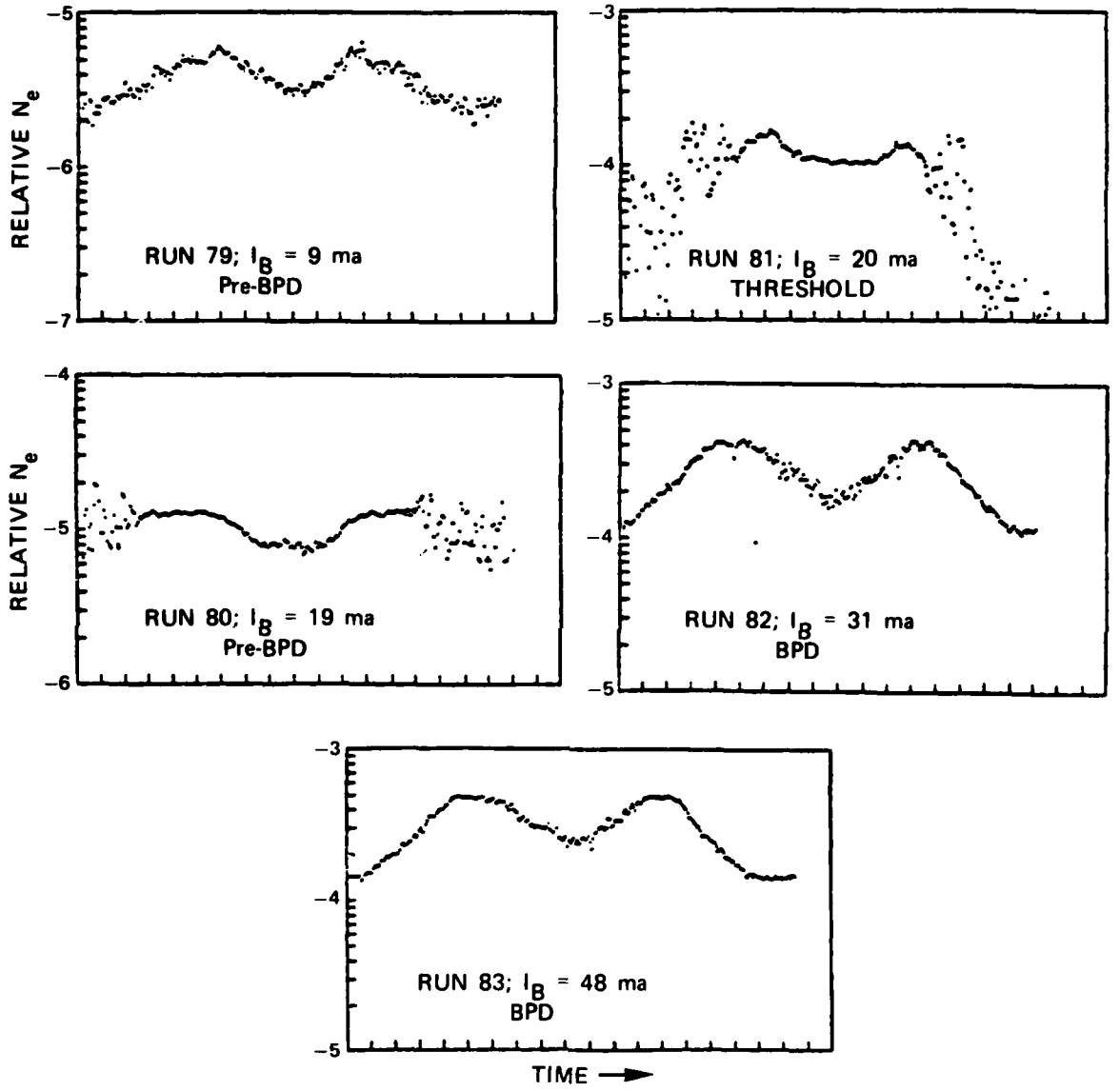
RELATIVE N_e
−5
−6
−7
RUN 79; I_B = 9 ma
Pre-BPD
−3
−4
−5
RUN 81; I_B = 20 ma
THRESHOLD
RELATIVE N_e
−4
−5
−6
RUN 80; I_B = 19 ma
Pre-BPD
−3
−4
−5
RUN 82; I_B = 31 ma
BPD
−3
−4
−5
RUN 83; I_B = 48 ma
BPD
TIME

(a)

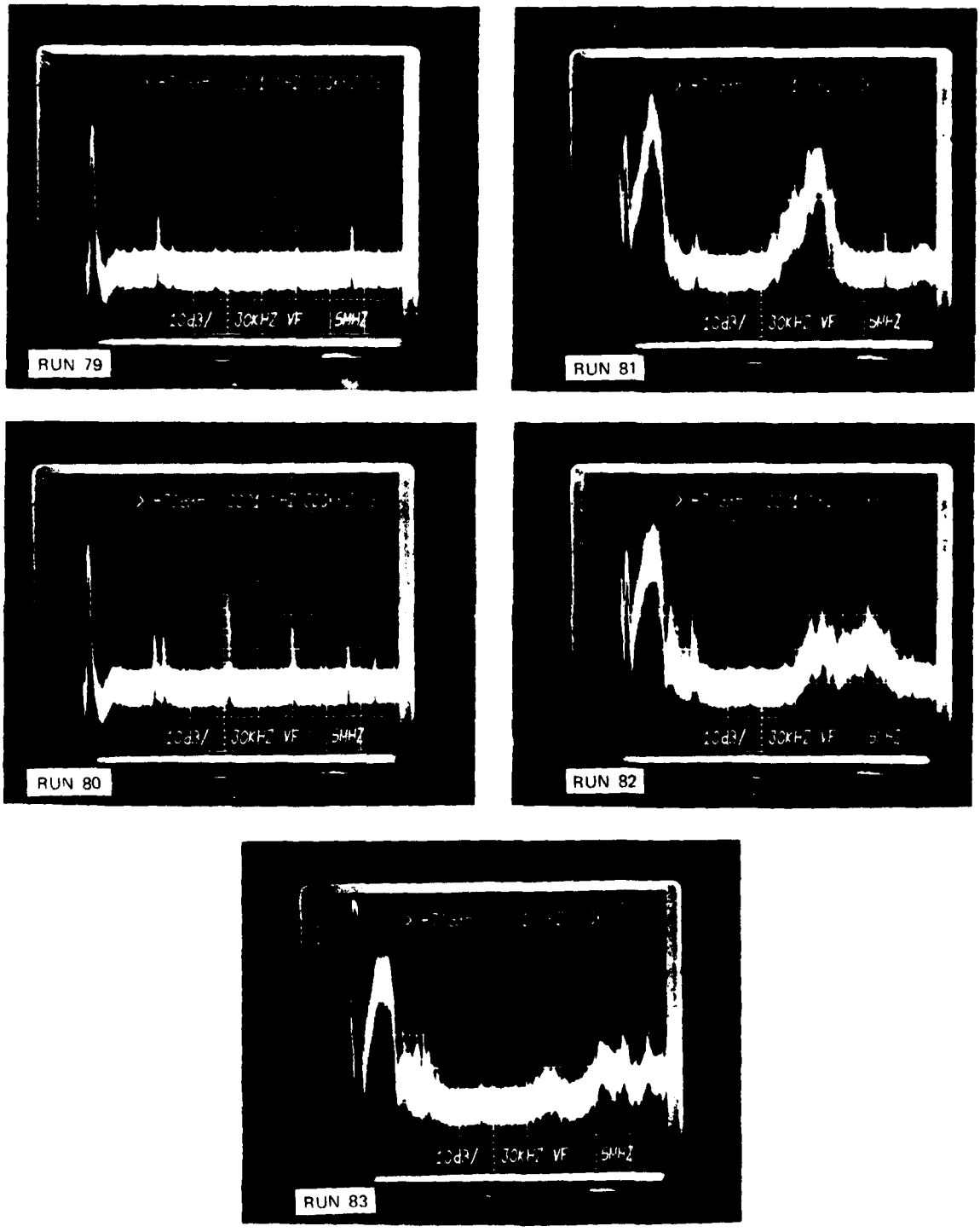

(b)

Fig. 6 – Sequence of relative plasma density profiles (Fig. 5A) and associated plasma wave signatures (Fig. 5B) for increasing values of beam current I_B at a fixed condition (V_BB) = (2.0 keV, 1.5g) encompassing runs 79 through 83 (pre-BPD through solid-BPD).

(It is important to note that the time-dependent photographs of the threshold RF spectrum, e.g., runs 57 and 81, erroneously indicate a solid-BPD spectrum and do not reflect the oscillations between the two beam-plasma states.) The conditions at threshold and under BPD are summarized in Table 1 where the peak density N_e^{max}, associated plasma frequency $2\pi\omega_p^{max}$, and plasma-to-cyclotron frequency ratio ω_p^{max}/ω_c are also listed. The results can be summarized by $\omega_p/\omega_c = 5.8^{+1.3}_{-1.9}$ as the density-dependent threshold condition for the BPD. As we will show in the next section, this result is consistent with a threshold model which assumes that BPD is triggered by the onset of a beam plasma instability.

It is proper to introduce one qualification regarding the experimentally determined values for ω_p/ω_c. By definition, they represent averages between two beam-plasma states (pre-and solid BPD). The consequence of this in the interpretation of the experimental values is merely one of definition. For example, if threshold were redefined as the maximum density under stable pre-BPD conditions (i.e., no oscillations into the solid-BPD state), then $\omega_p/\omega_c = 5.8$ would represent an upper limit. Our experience suggest that the "adjustment" in critical density would not be more than a factor of two less than the measured values. In this case we suggest that a more general statement of density-dependent threshold take the form

$$3.9 \lesssim \omega_p/\omega_c < 5.8. \qquad (4)$$

Before proceeding to the theoretical treatment it is appropriate to discuss several of the plasma density and wave-related features in the data presented in Figures 5 and 6.

Run 56 (upper left panel Figs. 5A and 5B) is very typical of a pre-BPD environment, in that the beam center (see e.g., Fig. 3) is well defined and of relatively narrow cross section, with an RF signature (upper left panel Fig.

TABLE 1. ABBREVIATED SUMMARY OF BEAM-PLASMA SURVEY

RUN #	BEAM-PLASMA STATE	ELECTRON GUN		CHAMBER CONDITION			N_e^{max}	f_c	f_p/f_c
		I_B (ma)	V_B(v)	B (g)	P (Torr)	THRUSTER			
40	THRESHOLD	37	1.9 (10^3)	0.9	0.7-1.5 (10^{-5})	ON	3.6 (10^6)	2.5 (10^6)	6.92
41	BPD	47	1.9 (10^3)	0.9	0.7-1.5 (10^{-5})	ON	5.6 (10^6)	2.5 (10^6)	8.60
48	THRESHOLD	34	1.9 (10^3)	0.9	0.7-1.5 (10^{-5})	OFF	3.3 (10^6)	2.5 (10^6)	6.6
49	BPD	45	1.9 (10^3)	0.9	0.7-1.5 (10^{-5})	OFF	5.0 (10^6)	2.5 (10^6)	8.12
57	THRESHOLD	18.5	1.3 (10^3)	0.9	0.7-1.5 (10^{-5})	OFF	1.5 (10^6)	2.5 (10^6)	4.45
58	BPD	28	1.3 (10^3)	0.9	0.7-1.5 (10^{-5})	OFF	4.5 (10^6)	2.5 (10^6)	7.71
63	THRESHOLD	7.8	800	0.9	0.84-1.5 (10^{-5})	OFF	0.98 (10^6)	2.5 (10^6)	3.7
64	BPD	9.9	800	0.9	0.84-1.5 (10^{-5})	OFF	2.6 (10^6)	2.5 (10^6)	5.9
69	THRESHOLD	6.2	800	0.9	0.7 (10^{-5})	ON	3.8 (10^6)	2.5 (10^6)	7.08
70	BPD	7.8	800	0.9	0.7 (10^{-5})	ON	3.6 (10^6)	2.5 (10^6)	6.89
81	THRESHOLD	20	2.0 (10^3)	1.5	0.6-1.2 (10^{-5})	OFF	7.0 (10^6)	3.7 (10^6)	6.65
82	BPD	30.5	2.0 (10^3)	1.5	0.6-1.2 (10^{-5})	OFF	1.8 (10^7)	3.7 (10^6)	10.7
86	THRESHOLD	12	1.3 (10^3)	1.5	0.6-1.2 (10^{-5})	OFF	3.9 (10^6)	3.7 (10^6)	4.96
87	BPD	18	1.3 (10^3)	1.5	0.6-1.2 (10^{-5})	OFF	1.1 (10^7)	3.7 (10^6)	8.34

5B) that is flat in character. At BPD threshold the beam-plasma system intermittently emits RF at and around the plasma frequency and the plasma expands in cross section (lower left panel Fig. 5A) eliminating the narrow beam profile characteristic of the pre-BPD state (Fig. 3 and 5A upper left). We note that the RF signatures are highly time dependent, generally fluctuating in intensity and in frequency. Similarly, the local plasma densities are highly time dependent (see e.g., I_B fluctuations in Fig. 4) with that dependency averaged over 1-sec intervals for the relative density profiles in Figs. 5 and 6.

As I_B is increased above the threshold level (Runs 58 and 59 in Figs. 5A and 5B) the plasma density increases and the radial profiles take-on variable configurations. In Run 58, for example, the beam center is "depleted" with an increased density level at its edges. This configuration has been observed in a number of cases and is thought to manifest electron heating in the beam core with generally higher diffusion rates and associated losses. The profile becomes more complex in Run 59, possibly due to higher order diffusion modes.

The results in Figure 6 have been selected to present information at a higher applied magnetic field and to illustrate that the description of beam-plasma profiles offered in connection with Figure 5 is by no means considered universally applicable to the various levels of the BPD. Our current level of understanding does not allow for a detailed cause-effect description of each and every profile but at present we would point to Figure 5A as the simplest configuration that illustrates the transition from pre- BPD to the solid BPD state.

III. THEORETICAL CONSIDERATIONS AND DISCUSSION OF RESULTS

Before presenting the theoretical details of the BPD threshold criteria as applied to the present experiment, it

is important to discuss some aspects of our model which play a key role in the interpretation of the experimental results.

For all experimental parameters the relevant mean free paths (i.e., thermalization, ionization, etc.) were much longer than the system length L. This, as discussed in detail by Papadopoulos (1981) for a finite system, leads to a requirement for axial confinement of both the ionizing and the ambient electrons. As shown in the above paper, the required axial confinement can be achieved, if the energy deposited by the beam electrons is absorbed by few ambient electrons (i.e., 1%) which are accelerated to energies larger than the ionization potential. A fraction of these electrons quickly escapes the system, thereby building potential sheaths at the ends. The sheaths accelerate ambient ions to escape at the rate of the fast electrons, while trapping the cold part of the energetic electron population. A detailed description of the process can be found in Papadopoulos (1981). For the purposes of the present paper we retain the requirement that the collisionless mechanism responsible for BPD should deposit most of its energy to suprathermal tails with energy much larger than the ionization energy while leaving the majority of the electrons cold. As discussed in many publications (Papadopoulos and Coffey 1974; Papadopoulos and Rowland 1978; Linson and Papadopoulos 1980; Papadopoulos 1981), this can be achieved if the frequency of the excited waves is near the electron plasma frequency ω_p, and the wave-energy $\frac{W}{N_e T_e}$ is greater than $k^2\lambda_D^2$, where W is the field energy density, N_e the ambient electron density, T_e the electron temperature, k the wave-number of the instability and λ_D the Debye length. In order for substantial $\frac{W}{N_e T_e}$ to be built in a finite length system the instability should be almost absolute. The dispersion relation for a beam plasma system is (Linson and Papadopoulos, 1980; Rowland et al., 1981)

$$k_z^2\left(1-\frac{\omega_p^2}{\omega^2}\right)+k_\perp^2\left(1-\frac{\omega_p^2}{\omega^2-\omega_c^2}\right)-k_z^2\frac{\alpha\omega_p^2}{(\omega-k_z v_b)^2}-k_\perp^2\frac{\alpha\omega_p^2}{(\omega-k_z v_b)^2-\omega_c^2}=0 \quad (5)$$

where $k_\perp^2 \equiv \frac{\Gamma_{s1}^2}{r_o^2}$ with Γ_{s1} the roots of the Bessel function $J_1(\Gamma_{s1}) = 0$ and r_o the beam radius. In Eq. (5), α is the beam-to-plasma density ratio, ω_p and ω_c the plasma and electron cyclotron frequencies, v_b the beam velocity and k_z the parallel wave number. On the basis of Eq. (5) we can find (Rowland et al., 1981) that an almost absolute instability can be excited near ω_e, for

$$\frac{k_\perp^2}{k_z^2} \leq 1 \quad (6)$$

Coupling this inequality with $k_z \approx \frac{\omega_p}{v_b}$ and $k_\perp = \frac{2.4}{r_o}$, gives our required threshold condition as

$$\omega_p^2 \geq \frac{(2.4)^2 v_b^2 \cos^2\theta}{r_o^2} \quad (7)$$

The criterion (7), with θ being the beam's angle of injection relative to the magnetic field, can be generalized to the case where the plasma radius R is different from the beam radius r_o (Rowland et al., 1981). In this case Eq. (7) becomes

$$\omega_p^2 \geq 2\frac{v_b^2 \cos^2\theta}{r_o^2 \ln(R/r_o)} \quad (8)$$

The value of r_o is given by considering both the Larmor radius as well as the term including space charge beam expansion (Linson and Papadopoulos, 1980). This gives

$$r_o = 2.1\frac{I_B^{1/2}}{BV_B^{1/4}}\left(\ln\frac{r_o}{r_g}+\frac{33}{\kappa}\sin^2\theta\right)^{1/2} \text{ m} \quad (9)$$

where κ is gun perveance in micropervs, r_g the gun radius in cm, I_B and V_B the beam current in amps and energy in keV,

and the magnetic field B is in gauss. From Eq. (8) and (9) and using $r_g \tilde{\sim} 2$mm and $\frac{r_o}{R} \tilde{\sim} \frac{1}{2}$ as observed we find

$$\frac{\omega_p}{\omega_c} \geq \frac{5\times10^{-1} V_B^{3/4}}{I_B^{1/2}} \quad \frac{\cos\theta}{(1 + \frac{8.5}{\kappa} \sin^2\theta)} \qquad (10)$$

We can see that the ω_p/ω_c ratio at threshold (with $\kappa \tilde{\sim} 1$ microperv) is rather insensitive to the beam injection angle for $\theta \lesssim 60^o$. In Table II we present the values of ω_p/ω_c computed on the basis of Eq. (10) by taking

$$\frac{\cos\theta}{(1 + \frac{8.5}{\kappa} \sin^2\theta)^{1/2}} \tilde{\sim} 1$$ for near parallel injection. From Table II we find the average computed value to be $\omega_p/\omega_c = 4.95$. This result, while subject to moderate uncertainties in r_o/R, is taken to be in excellent agreement with the experimentally derived conditions (Table 1 and Eq. 4) providing complementary arguments which confirm the original suggestion that the ignition of the BPD was strongly coupled to a density-dependent threshold criterion. We should mention that the above theory is consistent with the observational facts that the temperature of the electrons is much lower than the ionization potential (Szuszczewicz et al., 1979), while energetic tails are observed within the beam-plasma core (Szuszczewicz, 1980 unpublished).

TABLE II: COMPARISON BETWEEN THEORY AND EXPERIMENT

Run No.	V_B(keV)	I_B(ma)	ω_p/ω_c (calc.)	ω_p/ω_c (observed)
40	1.9	37	4.2	6.9
48	1.9	34	4.4	6.6
57	1.3	18.5	4.5	4.5
63	.8	7.8	4.7	3.7
69	.8	6.2	5.37	7.1
81	2	20	5.95	6.7
86	1.3	12	5.55	5.0

ACKNOWLEDGMENT

The various elements in this investigation were supported in whole or in part by NASA grant NAGW-69, Rice University subcontract NAS 8-33777-1, and NASA/NOAA Contract NA79RAE0039. Supplementary funding was also provided by the Office of Naval Research under Program Element 61153N-33 in Task Area RR033-02. We wish to thank J.C. Holmes for his critical care in electronics design of the P^3 instrumentation and L. Kegley for technical assistance in experiment execution.

REFERENCES

Bernstein, W., H. Leinbach, H. Cohen, P.S. Wilson, T.N. Davis, T. Hallinan, B. Baker, J. Martz, R. Zeimke, and W. Huber, "Laboratory observations of RF emissions at ω_{pe} and (N+1/2) ω_{CE} in electron beam-plasma and beam-beam interactions", J. Geophys. Res. 80, 4375, 1975.

Bernstein, W., H. Leinbach, P. Kellogg, S. Monson, T. Hallinan, O.K. Garriott, A. Konradi, J. McCoy, P. Daly, B. Baker, and H.R. Anderson, "Electron beam injection experiments: The beam-plasma discharge at low pressures and magnetic field strengths", Geophys. Res. Lett. 5, 127, 1978.

Bernstein, W., H. Leinbach, P.J. Kellogg, S.J. Monson and T. Hallinan, "Further laboratory measurements of the beam-plasma discharge", J. Geophys. Res. 84, 7271, 1979.

Bernstein, W., B.A. Whalen, F.R. Harris, A.G. McNamara and A. Konradi, "Laboratory studies of the charge neutralization of a rocket payload during electron beam emission", Geophys. Res. Lett. 7. 93, 1980.

Cambou, F., V.S. Dokoukine, V.N. Ivchenko, G.G. Managadze, V.V. Migulin, O.K. Nazarenko, A.T. Nesmyanovich, A.Kh. Pyatsi, R.Z. Sagdeev and I.A. Zhulin, "The Zarnitza rocket experiment on electron injection", Space Research XV, 491-500, Akademie-Verlag, Berlin 1975.

Cambou, F., J. Lavergnat, V.V. Migulin, A.I. Morozov, B.E. Paton, R. Pellat, A. Pyatsi, H. Reme, R.Z. Sagdeev, W.R. Sheldon and I.A. Zhulin, "ARAKS-Controlled or puzzling experiment"? Nature 271, 723, 1978.

Chen, F.F., in Plasma Diagnostic Techniques, Ch. 4, edited by R.H. Huddlestone and S.L. Leonard, Academic, New York 1965.

Getty, W.D. and L.D. Smullin, "Beam-plasma discharge: Buildup of oscillations," J. Appl. Phys. 34, 3421, 1963.

Hendrickson, R.A. and J.R. Winckler, "Echo III: The study of electric and magnetic fields with conjugate echoes from artificial electron beams injected into the auroral zone ionosphere", Geophys. Res. Lett., 3, 409, 1976.

Hess, W.N., M.C. Trichel, T.N. Davis, W.C. Beggs, G.E. Kraft, E. Strasinopoulos, and E.J.R. Maier, "Artificial aurora experiment: Experiment and principal results". Geophys. Res., 76, 6067, 1971.

Holmes, J.C. and E.P. Szuszczewicz, "A versatile plasma probe", Rev. Sci. Instr. 46, 592, 1975.

Holmes, J.C. and E.P. Szuszczewicz, "A plasma probe system with automatic sweep adjustment", Rev. Sci. Instr., 52, 377, 1981.

Jost, R.J., H.R. Anderson and J.O. McGarity, "Measured electron energy distributions during electron beam-plasma interactions", Geophys. Res. Lett. 7, 509, 1981.

Linson, L.M. and K. Papadopoulos, "Review of the status of theory and experiment for injection of energetic electron beams in space", Rpt. LAPS-69/SAI-D23-459-LJ, (April 1980).

Monson, S.J. and P.J. Kellogg, "Ground observations of waves at 2.96 MHz generated by an 8- to 40-KEV electron beam in the ionosphere", J. Geophys. Res., 83, 121, 1978.

Papadopoulos, K., "Theory of beam plasma discharge", Proc. NATO Advanced Research Institute on Artificial Particle Beams in Space Plasma Physics", (Geilo, Norway 1981 (in press).

Papadopoulos, K. and H.L. Rowland, "Collisionless effects on the spectrum of secondary auroral electrons at low altitudes", J. Geophys. Res. 83, 5768, 1978.

Papadopoulos, K. and T. Coffey, "Nonthermal features of the auroral plasma due to precipitating electrons", J. Geophys. Res., 79, 674, 1974a.

Papadopoulos, K. and T. Coffey, "Anomalous resistivity in the auroral plasma", J. Geophys. Res., 79, 1558, 1974b.

Rowland, H.L., C.L. Chang and K. Papadopoulos, "Scaling of the beam-plasma discharge", J. Geophys. Res., (1981, in press).

Szuszczewicz, E.P. and J.C. Holmes, "Surface contamination of acive electrodes in plasmas: Distortion of conventional Langmuir probe measurements", J. Appl. Phys. 46, 5134, 1975.

Szuszczewicz, E.P. and J.C. Holmes, "Reentry plasma diagnostics with a pulsed plasma probe", AIAA Paper No. 76-393, AIAA 9th Fluid and Plasma Dynamics Conference (San Diego, CA/July 1976).

Szuszczewicz, E.P. and J.C. Holmes, "Observations of electron temperature gradients in mid-latitude E_s layers", J. Geophys. Res., 82, 5073, 1977.

Szuszczewicz, E.P., D.N. Walker and H. Leinbach, "Plasma diffusion in a space-simulation beam-plasma-discharge", Geophys. Res. Lett. 6, 201, 1979.

Winckler, J.R., R.L. Arnoldy and R.A. Hendrickson, "Echo 2: A study of electron beams injected into the high-latitude ionosphere from a large sounding rocket", J. Geophys. Res., 80, 2083, 1975.


DATE
ILME